Dual Correlation-aware Mamba for Microvascular Obstruction Identification in Non-contrast Cine Cardiac Magnetic Resonance

Yige Yan[1⋆], Jun Cheng[2(✉)], Xulei Yang[2], Shuang Leng[3,4], Ru San Tan[3,4], Liang Zhong[3,4(✉)], and Jagath C. Rajapakse[1]

[1] College of Computing and Data Science, Nanyang Technological University, Singapore
asjagath@ntu.edu.sg
[2] Institute for Infocomm Research, Agency for Science, Technology and Research (A*STAR), 1 Fusionopolis Way, Connexis, 138632, Singapore
cheng_jun@i2r.a-star.edu.sg
[3] National Heart Centre Singapore, 5 Hospital Drive, 169609, Singapore
[4] Duke-NUS Medical School, National University of Singapore, Singapore
gmszl@nus.edu.sg

Abstract. Microvascular obstruction (MVO) is a key prognostic factor in acute myocardial infarction, with affected patients experiencing higher mortality rates. Currently, late gadolinium enhancement cardiac magnetic resonance (CMR) is the gold standard for MVO identification. However, it is unsuitable for patients with renal impairment, who make up 20% of all patients. Recent studies have demonstrated the feasibility of using non-contrast cine CMR to identify MVO. Despite this, existing methods struggle to effectively learn crucial motion features, as they implicitly model motion dynamics while overlooking regional wall motion abnormalities, which are important for MVO identification. To this end, we introduce a Dual Correlation-aware Mamba, which includes an Adjacent Frame Correlation (AFC) module and a Diastolic Frame Correlation (DFC) module to address these limitations. The AFC module calculates the correlations through adjacent frames to explicitly model the motion dynamics. The DFC module learns correlations between the diastolic frame and others. Leveraging the diastolic frame as a reference, this module highlights regional abnormalities and guides motion learning. Experimental results demonstrate that our method outperforms competing methods, potentially providing a non-contrast tool for MVO identification. The code is available at https://github.com/code-koukai/Dual-Correlation-Mamba.

Keywords: Cardiac Magnetic Resonance · Microvascular Obstruction · Contrast-free Technology · Motion Features.

⋆ The work was done during an internship at I^{2}R, A*STAR.

1 Introduction

Acute myocardial infarction remains a leading cause of death worldwide [3]. Microvascular obstruction (MVO), a frequent complication, is strongly linked to increased mortality and serves as a critical prognostic indicator [10]. Clinically, identifying the presence of MVO is essential for initial risk stratification and guiding treatment strategies [21]. Late gadolinium enhancement (LGE) cardiac magnetic resonance (CMR) is the gold standard for MVO identification [1,19]. However, it is unsuitable for patients with renal impairment, who make up 20% of cases [20]. Therefore, there is an increasing need for non-contrast MVO identification. Cine CMR, a non-contrast dynamic imaging technique, has emerged as a promising alternative [5,7,16]. It captures motion throughout the cardiac cycle, enabling the detection of regional wall motion abnormalities (RWMA) and myocardial dysfunction associated with MVO [6]. These findings highlight the potential of cine CMR for non-contrast MVO identification [8,28,29].

In cine CMR, MVO is not visible on a single frame due to the absence of contrast agents, making it necessary to analyze motion across multiple frames for its identification. Some studies have leveraged motion analysis in cine CMR to assess myocardial function and pathology [11,14,17,23,24,26]. However, the inherent complexity and small size of MVO motion complicate the analysis, making identification more challenging. Yan *et al.* [27] demonstrate the feasibility of MVO identification in cine CMR by extracting spatiotemporal features. However, this method implicitly models motion dynamics, failing to sufficiently capture the motion feature. Furthermore, they overlook the RWMA induced by MVO, which is crucial for MVO identification in cine CMR.

In this paper, we propose a Dual Correlation-aware Mamba (DCM), which includes an Adjacent Frame Correlation (AFC) module and a Diastolic Frame Correlation (DFC) module to address these issues. Our contributions lie in explicitly modeling motion dynamics while leveraging the diastolic frame as a reference to guide motion learning. Specifically, to explicitly model the motion dynamics, the AFC module computes correlations between adjacent frames to estimate pixel displacements. The features are enhanced by displacement estimation and aggregated by a bidirectional temporal Mamba [9]. Inspired by the important role of RWMA in MVO diagnosis [15,25], the DFC module designates the diastolic frame as a reference, highlighting RWMA variations throughout the cardiac cycle. It learns correlations between the diastolic frame and the other frames and aggregates the motion information through a bidirectional spatial Mamba. Experiments demonstrate that our proposed method enhances motion feature extraction, leading to improved non-contrast MVO identification. The key contributions of our work are as follows:

1. We introduce Dual Correlation-aware Mamba, a novel method for MVO identification that explicitly models motion dynamics and guides motion learning to enhance motion feature extraction in non-contrast cine CMR;
2. Our proposed method includes the Adjacent Frame Correlation module to explicitly model the motion by computing correlations between adjacent

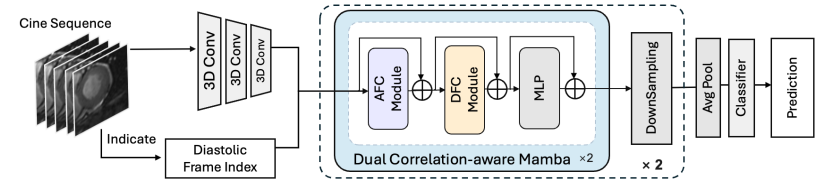

(a) Overview of our framework

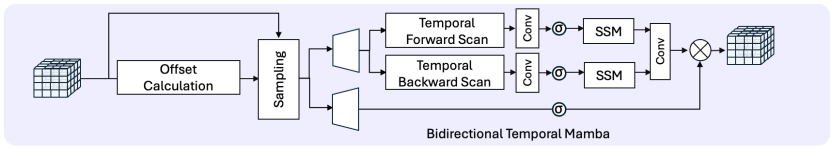

(b) Details of Adjacent Frame Correlation (AFC) module

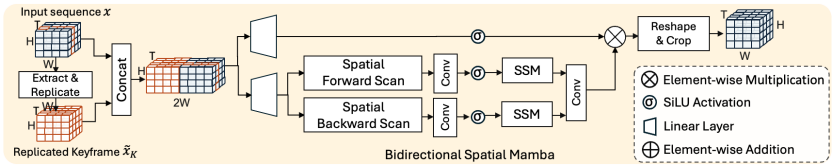

(c) Details of Diastolic Frame Correlation (DFC) module

Fig. 1: The illustration of our method includes: (a) the overview of our framework, (b) the details of the Adjacent Frame Correlation module, and (c) the details of the Diastolic Frame Correlation module.

frames, and the Diastolic Frame Correlation module to guide motion learning by learning correlations between the diastolic frame and the other frames;

3. Experiment results demonstrate that our method outperforms competing methods, effectively enhancing motion feature extraction and offering a novel non-contrast solution for MVO identification.

2 Method

We propose a novel framework for non-contrast MVO identification that computes the correlations between adjacent frames and learns the correlations between the diastolic frame and others to enhance motion feature extraction using non-contrast cine CMR. The model, illustrated in Fig. 1a, extracts features from a cine sequence using three 3D CNN layers. These features are refined using Dual Correlation-aware Mamba (DCM) blocks, each comprising an Adjacent Frame Correlation (AFC) module and a Diastolic Frame Correlation (DFC) module, to enhance motion extraction. The DFC module leverages the diastolic frame index to locate the diastolic frame. Two DCM blocks and a downsampling layer form a stage, with features processed through two sequential stages for progressive learning. Finally, the features undergo average pooling and a classifier layer to generate the prediction for the presence of MVO.

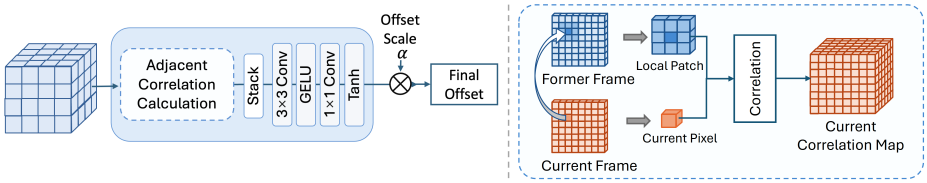

(a) Offset Calculation module (b) Adjacent Correlation Calculation

Fig. 2: Details of (a) Offset Calculation module and (b) Adjacent Correlation Calculation. Adjacent Correlation Calculation uniformly processes adjacent frame pairs along the temporal dimension and stacks the results.

2.1 Dual Correlation-aware Mamba

MVO identification in cine CMR is challenging due to the induced complex motion and its small size. Existing methods implicitly model motion, leading to inadequate motion extraction. They also overlooked the crucial RWMA associated with MVO. We propose a Dual Correlation-aware Mamba, which includes an AFC module for explicit motion modeling and a DFC module to guide the model's motion learning on motion abnormalities to address these limitations.

The AFC module predicts displacement offsets between adjacent frames, explicitly modeling motion representation. The processed features are then passed to the DFC module for enhanced motion learning. The DFC module utilizes the diastolic frame as a global reference for the other frames, guiding the model's motion learning. Finally, the fused features are fed into an MLP, which performs nonlinear transformation to further refine the overall feature representation. A residual connection is applied after each module.

Adjacent Frame Correlation Module Existing methods implicitly model motion in cine CMR while lacking dedicated mechanisms to focus on motion learning, resulting in insufficient motion extraction. However, motion extraction plays a crucial role in MVO identification. In light of this, we propose the AFC module, which explicitly models cardiac motion by computing correlations between adjacent frames, enhancing the model's motion extraction capabilities.

Fig. 1b illustrates the details of the AFC module. Given an input sequence $X \in \mathbb{R}^{B\times C\times T\times H\times W}$ (where B is the batch size, C the channels, T the time steps, and H and W the height and width), we first feed it into the Offset Calculation module, which is depicted in Fig. 2a. Specifically, we extract adjacent frame pairs X_i and $X_{i+1} \in \mathbb{R}^{B\times C\times H\times W}$ for each frame index $i \in \{1, \ldots, T-1\}$. For each pair, we compute local adjacent correlations within a symmetric window $W = \{(\Delta h, \Delta w) \mid \Delta h, \Delta w \in [-r, r]\}$, as illustrated in Fig. 2b:

$$\mathrm{Corr}_i(b, h, w, \Delta h, \Delta w) = \frac{\langle X_{i+1}(b, \cdot, h, w),\ X_i(b, \cdot, h+\Delta h, w+\Delta w)\rangle}{\sqrt{C}}, \quad (1)$$

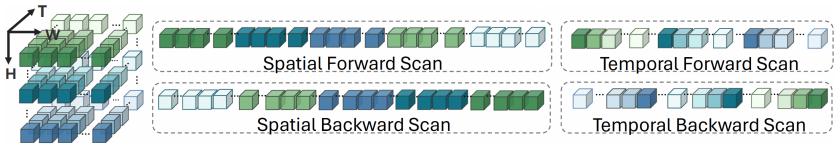

Fig. 3: Illustration of the bidirectional spatial and temporal scans. The arrangements of differently colored blocks illustrate the scanning orders.

where r is the window radius and $\langle \cdot, \cdot \rangle$ denotes the inner product. The resulting Corr_i of shape $[B, H, W, 2r+1, 2r+1]$ is reshaped into $\hat{\mathrm{Corr}}_i \in \mathbb{R}^{B\times(2r+1)^2\times H\times W}$ and fed into a network $f(\cdot)$, which consists of two convolutional layers with GELU activation, to predict offsets:

$$dh, dw = \alpha \cdot \tanh\Big(f\big(\hat{\mathrm{Corr}}_i\big)\Big), \tag{2}$$

where α is a offset scale factor and $dh, dw \in \mathbb{R}^{B\times H\times W}$ are predicted offsets. Here, we set $\alpha = 3$. Using bilinear interpolation, the features are resampled based on the dh and dw, yielding the final aligned feature representation:

$$\hat{X}_i(b, \cdot, h, w) = \mathcal{I}\big(X_i,\ h + dh(b, h, w), w + dw(b, h, w)\big), \tag{3}$$

where $\mathcal{I}(\cdot)$ denotes the interpolation function. Next, we employ bidirectional temporal Mamba for aggregation. We stack $\hat{X}_i$ temporally and perform temporal forward and backward scans, as illustrated in Fig. 3, forming two sequences. These sequences are then processed using selective state space models (SSMs) [9] and fused to obtain the final representation. This approach explicitly models myocardial motion, enhancing motion modeling effectiveness.

Diastolic Frame Correlation Module Existing methods overlook the RWMA caused by MVO, missing its value for MVO identification. We propose the DFC module, as depicted in Fig. 1c, to learn frame-to-frame correlations using the diastolic frame as a reference. This approach is motivated by the diastole's characteristics since its minimal myocardial wall thickness and clear cardiac structure provide a reference for comparing frames, emphasizing the manifestation of RWMA throughout the cardiac cycle. Specifically, we use diastolic frames from either the end-diastolic phase or those adjacent to it to ensure a clear reference.

Given an input sequence $x \in \mathbb{R}^{B\times C\times T\times H\times W}$, we extract the diastolic frame as the keyframe x_K and replicate it along the temporal dimension to obtain $\tilde{x}_K$. Then $\tilde{x}_K$ is concatenated with x along the width dimension, forming a joint representation $x_{\text{joint}} \in \mathbb{R}^{B\times C\times T\times H\times(2W)}$. Next, x_{joint} undergoes spatial forward and backward scans to generate bidirectional sequences, as shown in Fig. 3. These sequences are processed by SSMs to establish global correspondences between each frame and the keyframe. Finally, the features are reshaped to their original form, with the last W elements along the width dimension extracted as the final feature. In this way, we can build a diastole-focused correlation comparison, which highlights how cardiac motion evolves relative to the diastolic frame.

Table 1: Performance Comparison with Competing Methods

Model	AUC	Specificity	Accuracy	Recall	F1-score	Params
VST[12]	0.5878	0.5714	0.5413	0.5000	0.4786	27.58M
VIVIT[2]	0.5571	0.5974	0.5413	0.4642	0.4602	41.98M
TimesFormer[4]	0.5797	0.5389	0.5226	0.5000	0.4686	76.54M
TAM[13]	0.6372	0.6818	0.6241	0.5446	0.5495	24.80M
P3D[18]	0.6321	0.6627	0.6385	0.5909	0.5253	43.72M
C3D[22]	0.6140	0.5779	0.5677	0.5536	0.5188	63.32M
CGMR[27]	0.7231	0.7337	0.6842	0.6161	0.6216	43.72M
Our Method	**0.7687**	**0.7532**	**0.7218**	**0.6786**	**0.6726**	39.91M

2.2 Loss Function

To train our model for MVO identification, we use the cross-entropy (CE) loss for classification with coarse-grained mask regularization [27] and mean square error (MSE) loss. The total loss is defined as:

$$L_{total} = L_{\text{CE}} + \lambda \cdot L_{\text{MSE}}, \tag{4}$$

where L_{CE} is the CE loss, L_{MSE} is the MSE loss, and λ is a weighting factor balancing the two loss components. Based on the work [27], we set $\lambda = 0.05$.

3 Experimental Results

3.1 Dataset and Metrics

The dataset includes 816 cases from acute myocardial infarction patients, acquired with a 3T Siemens scanner from local hospitals. Each case contains a cine sequence and an LGE-derived MVO annotation. The dataset was randomly split into training (550 cases, 221 MVO-positive) and test (266 cases, 112 MVO-positive) sets. We evaluated our model's performance using Area Under Curve (AUC), Specificity, Accuracy, Recall, and F1-score.

3.2 Implementation Details

We trained the model for 10K iterations with a batch size of 8, using AdamW optimizer with an initial learning rate of 1E-5. The learning rate was scheduled using a linear warm-up for the first 1,500 iterations, followed by a polynomial decay policy with power 1.0 until iteration 10K. All models are trained on an Nvidia A100 GPU. A fixed random seed was set. Data augmentation was used, including flipping, blurring, and noise addition.

3.3 Performance Comparison with Competing Methods

Since non-contrast MVO identification is still in the early stages with limited research, we compared our model against competing methods, including CGMR

Table 2: Ablation Study of the Proposed Modules

AFC	DFC	AUC	Specificity	Accuracy	Recall	F1-score	Params
✓	✓	**0.7687**	**0.7532**	**0.7218**	**0.6786**	**0.6726**	39.91M
	✓	0.7439	0.7273	0.7030	0.6696	0.6550	38.54M
✓		0.7378	0.7273	0.7068	0.6786	0.6609	38.95M
		0.7312	0.7142	0.6992	0.6786	0.6556	37.58M

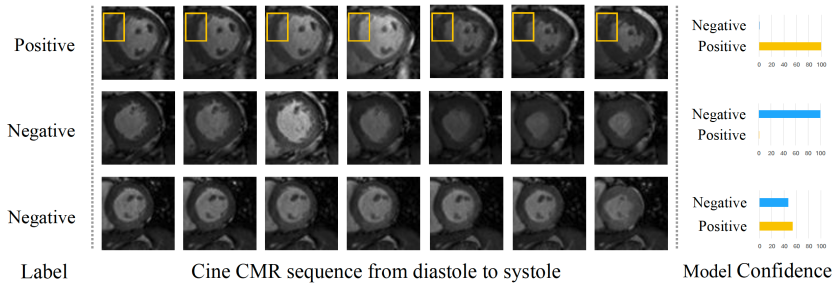

Fig. 4: Examples for good and bad cases. The first two examples show successful cases, while the last displays a failed case. The cine sequences highlight diastole-to-systole dynamics, with the leftmost frames in diastole and the rightmost frames in systole. Yellow boxes indicate the locations of MVOs.

[27] and other computer vision approaches, as summarized in Table 1. Results show our approach effectively identifies the presence of MVO, achieving an AUC of 0.7687 and surpassing competing methods. Fig. 4 illustrates that our model can accurately identify MVO in most cases. However, individual variability causes some non-MVO cases to exhibit motion patterns similar to those induced by MVO, making identification challenging.

3.4 Ablation Studies

Ablation Study of the Proposed Modules We evaluated the impact of our proposed modules on overall performance using four configurations: (1) the full framework, (2) without the AFC module, (3) without the DFC module, and (4) without both. In these experiments, the AFC module was replaced with a bidirectional temporal Mamba, while the DFC module was substituted with a bidirectional spatial Mamba. As shown in Table 2, both modules contribute to the performance. Replacing Mamba with the self-attention mechanism resulted in an AUC of 0.7150, demonstrating the effectiveness of our design.

Ablation Study of the Adjacent Frame Correlation Module Table 3 presents the impact of AFC settings on performance. The results indicate that both an optimal radius and learnable offsets improve performance. Additionally, we visualized the AFC module's motion modeling, as shown in Fig. 5.

Keyframe Selection Ablation We investigated the effect of keyframe selection in the DFC module. For clarity, the entire cardiac cycle was linearly scaled to the

Table 3: Ablation Study of the Adjacent Frame Correlation Module

Settings	AUC	Specificity	Accuracy	Recall	F1-score
Radius=[1,1]	0.7451	0.7208	0.6955	0.6607	0.6463
Radius=[2,1]	**0.7687**	**0.7532**	**0.7218**	**0.6786**	**0.6726**
Radius=[3,1]	0.7583	0.7467	0.7180	0.6786	0.6691
Fixed Offset	0.7227	0.6753	0.6729	0.6696	0.6329

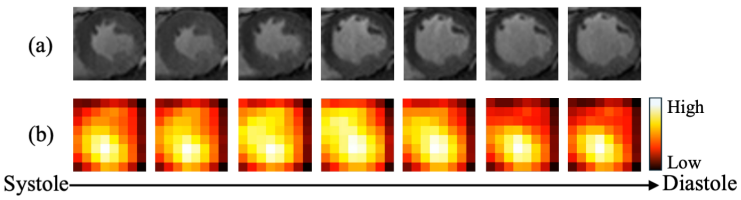

Fig. 5: Visualization of the magnitude of (dh, dw) in Offset Calculation module. (a) shows the cine CMR from the systole to the diastole, and (b) presents the corresponding heatmap. The heatmap effectively captures myocardial motion degrees from systole to diastole, which are initially low, then increase over time, and eventually decrease.

interval [0, 1], with 0 marking the start of the cycle and 1 representing the end-diastolic (or near end-diastolic) phase. Keyframes chosen at 1/6, 1/2, and 2/3 were compared with using the frame at 1. Fig. 6a demonstrates the importance of selecting the end-diastolic or near end-diastolic frame as the keyframe.

Number of Stages Ablation We investigated the impact of the number of stages on our framework. Fig. 6b shows that selecting two stages achieves the best performance.

4 Conclusion

This paper introduces a Dual Correlation-aware Mamba for MVO identification in non-contrast cine CMR, including an Adjacent Frame Correlation module to explicitly model the dynamics and a Diastolic Frame Correlation module to guide motion learning. Results indicate our method enhances motion feature extraction and outperforms competing methods. Future work will refine MVO delineation and distinguish it from other cardiac lesions causing myocardial abnormalities.

Acknowledgments. This research work is supported by the Agency for Science, Technology and Research (A*STAR) under its MTC Programmatic Funds (Grant No. M23L7b0021). It is also supported by the Interdisciplinary Graduate Programme (IGP) at Nanyang Technological University.

Disclosure of Interests. The authors have no competing interests to declare that are relevant to the content of this article.

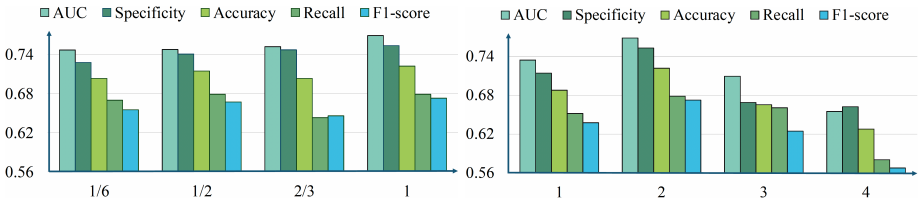

(a) Keyframe Selection Ablation (b) Number of Stages Ablation

Fig. 6: Visualization of performance comparison with (a) different keyframe selection and (b) different number of stages.

References

1. Amyar, A., Nakamori, S., Morales, M., Yoon, S., Rodriguez, J., Kim, J., Judd, R.M., Weinsaft, J.W., Nezafat, R.: Gadolinium-free cardiac mri myocardial scar detection by 4d convolution factorization. In: International Conference on Medical Image Computing and Computer-Assisted Intervention. pp. 639–648. Springer (2023)
2. Arnab, A., Dehghani, M., Heigold, G., Sun, C., Lučić, M., Schmid, C.: Vivit: A video vision transformer. In: Proceedings of the IEEE/CVF international conference on computer vision. pp. 6836–6846 (2021)
3. Barnes, M., Heywood, A.E., Mahimbo, A., Rahman, B., Newall, A.T., Macintyre, C.R.: Acute myocardial infarction and influenza: a meta-analysis of case–control studies. Heart **101**(21), 1738–1747 (2015)
4. Bertasius, G., Wang, H., Torresani, L.: Is space-time attention all you need for video understanding? In: Proceedings of the 38th International Conference on Machine Learning. vol. 2, p. 4 (2021)
5. Bi, N., et al.: Segmorph: Concurrent motion estimation and segmentation for cardiac mri sequences. IEEE transactions on medical imaging (2024)
6. Choy, C.H., Steeds, R.P., Leyva, F., Moody, W.E.: The spectrum of microvascular obstruction in nonischemic cardiomyopathy. Cardiovascular Imaging **15**(12), 2139–2144 (2022)
7. Cui, H., Li, Y., Wang, Y., Xu, D., Wu, L.M., Xia, Y.: Towards accurate cardiac mri segmentation with variational autoencoder-based unsupervised domain adaptation. IEEE Transactions on Medical Imaging (2024)
8. Gräni, C., Stark, A.W., Fischer, K., et al.: Diagnostic performance of cardiac magnetic resonance segmental myocardial strain for detecting microvascular obstruction and late gadolinium enhancement in patients presenting after a st-elevation myocardial infarction. Frontiers in cardiovascular medicine **9**, 909204 (2022)
9. Gu, A., Dao, T.: Mamba: Linear-time sequence modeling with selective state spaces. arXiv preprint arXiv:2312.00752 (2023)
10. Hamirani, Y.S., Wong, A., Kramer, C., Salerno, M.: Effect of microvascular obstruction and intramyocardial hemorrhage by cmr on lv remodeling and outcomes after myocardial infarction: a systematic review and meta-analysis. JACC. Cardiovascular imaging **7 9**, 940–52 (2014)
11. Liu, X., et al.: Tagged-to-cine mri sequence synthesis via light spatial-temporal transformer. In: International Conference on Medical Image Computing and Computer-Assisted Intervention. pp. 701–711. Springer (2024)

12. Liu, Z., Ning, J., Cao, Y., Wei, Y., Zhang, Z., Lin, S., Hu, H.: Video swin transformer. In: Proceedings of the IEEE/CVF conference on computer vision and pattern recognition. pp. 3202–3211 (2022)
13. Liu, Z., Wang, L., Wu, W., Qian, C., Lu, T.: Tam: Temporal adaptive module for video recognition. In: Proceedings of the IEEE/CVF international conference on computer vision. pp. 13708–13718 (2021)
14. Meng, Q., Bai, W., Liu, T., O'regan, D.P., Rueckert, D.: Mesh-based 3d motion tracking in cardiac mri using deep learning. In: International Conference on Medical Image Computing and Computer-Assisted Intervention. pp. 248–258. Springer (2022)
15. Nijveldt, R., Beek, A.M., Hirsch, A., et al.: Functional recovery after acute myocardial infarction: comparison between angiography, electrocardiography, and cardiovascular magnetic resonance measures of microvascular injury. Journal of the American College of Cardiology **52**(3), 181–189 (2008)
16. Qi, R., Li, X., Xu, L., Zhang, J., Zhang, Y., Xu, C.: Cardiac physiology knowledge-driven diffusion model for contrast-free synthesis myocardial infarction enhancement. In: International Conference on Medical Image Computing and Computer-Assisted Intervention. pp. 200–210. Springer (2024)
17. Qiu, J., Li, L., Wang, S., Zhang, K., Chen, Y., Yang, S., Zhuang, X.: Myops-net: Myocardial pathology segmentation with flexible combination of multi-sequence cmr images. Medical image analysis **84**, 102694 (2023)
18. Qiu, Z., Yao, T., Mei, T.: Learning spatio-temporal representation with pseudo-3d residual networks. In: Proceedings of the IEEE/CVF international conference on computer vision. pp. 5533–5541 (2017)
19. Reimer, K.A., Lowe, J.E., Rasmussen, M.M., Jennings, R.B.: The wavefront phenomenon of ischemic cell death. 1. myocardial infarct size vs duration of coronary occlusion in dogs. Circulation **56**(5), 786–794 (1977)
20. Shroff, G.R., Frederick, P.D., Herzog, C.A.: Renal failure and acute myocardial infarction: clinical characteristics in patients with advanced chronic kidney disease, on dialysis, and without chronic kidney disease. American heart journal **163**(3), 399–406 (2012)
21. Symons, R., Pontone, G., Schwitter, J., et al.: Long-term incremental prognostic value of cardiovascular magnetic resonance after st-segment elevation myocardial infarction: a study of the collaborative registry on cmr in stemi. JACC: Cardiovascular Imaging **11**(6), 813–825 (2018)
22. Tran, D., Bourdev, L., Fergus, R., Torresani, L., Paluri, M.: Learning spatiotemporal features with 3d convolutional networks. In: Proceedings of the IEEE/CVF international conference on computer vision. pp. 4489–4497 (2015)
23. Tripathi, P.C., Suvon, M.N., Schobs, L., Zhou, S., Alabed, S., Swift, A.J., Lu, H.: Tensor-based multimodal learning for prediction of pulmonary arterial wedge pressure from cardiac mri. In: International Conference on Medical Image Computing and Computer-Assisted Intervention. pp. 206–215. Springer (2023)
24. Vimalesvaran, K., Uslu, F., Zaman, S., Galazis, C., Howard, J., Cole, G., Bharath, A.A.: Detecting aortic valve pathology from the 3-chamber cine cardiac mri view. In: International Conference on Medical Image Computing and Computer-Assisted Intervention. pp. 571–580. Springer (2022)
25. Wu, K.C.: Cmr of microvascular obstruction and hemorrhage in myocardial infarction. Journal of Cardiovascular Magnetic Resonance **14**(1), 72 (2012)
26. Xu, C., Xu, L., Ohorodnyk, P., Roth, M., Chen, B., Li, S.: Contrast agent-free synthesis and segmentation of ischemic heart disease images using progressive sequential causal gans. Medical image analysis **62**, 101668 (2020)

27. Yan, Y., Cheng, J., Yang, X., Gu, Z., Leng, S., Tan, R.S., Zhong, L., Rajapakse, J.C.: Coarse-grained mask regularization for microvascular obstruction identification from non-contrast cardiac magnetic resonance. In: International Conference on Medical Image Computing and Computer-Assisted Intervention. pp. 231–241. Springer (2024)
28. Zhang, Q., Burrage, M.K., Shanmuganathan, M., et al.: Artificial intelligence for contrast-free mri: scar assessment in myocardial infarction using deep learning–based virtual native enhancement. Circulation **146**(20), 1492–1503 (2022)
29. Zhu, Y., Cheng, J., Cui, Z.X., Ren, J., Wang, C., Liang, D.: Sre-cnn: A spatiotemporal rotation-equivariant cnn for cardiac cine mr imaging. In: International Conference on Medical Image Computing and Computer-Assisted Intervention. pp. 679–689. Springer (2024)